# APPLICATION OF DISTRIBUTED AUTOMATED MDO ENVIRONMENT TO AERO/ACOUSTIC SHAPE OPTIMIZATION OF A FAN BLADE

**U. Idahosa\* and V. V. Golubev[†]**
Embry-Riddle Aeronautical University, FL
**V.O. Balabanov[‡]**
VR&D, Inc., CO

## ABSTRACT

This work discusses application of an automated multi-disciplinary design optimization (MDO) system to noise control in turbomachinery. Numerous issues in the automated optimization procedure, such as those related to proper geometry parameterization, algorithms selection, and transparent interconnections between different elements of the optimization process are discussed. In benchmark test studies, the work examines a problem of blade shape optimization to minimize fan (rotor) noise, the dominant source of sound radiation both in high-speed fan applications (such as high-bypass-ratio turbofans, propellers of turboprop and IC engines in general aviation, and helicopter rotors) and low-speed ones (including applications in automotive, computer, air-conditioning and other industries). For low-speed fan applications, an approach is developed based on using an unstructured RANS solver coupled with an automated mesh generator. In the high-speed open-rotor project, the automated optimal blade design process employs a response analysis module developed on the basis of panel-based aerodynamic code integrated with an integral acoustic solver. Success of various optimization algorithms (including gradient-based and evolutionary) in finding global minima of the objective function for a noise metric in both unconstrained and constrained optimization processes is examined.

## INTRODUCTION

Efforts to merge MDO and CFD technologies have become a recent trend in the conceptual aircraft design: as was originally stated in Ref. [1], with the availability of high performance computing platforms and robust numerical methods to simulate fluid flows, it is possible to shift attention from CFD development to automated design procedures which combine CFD with optimization techniques to determine optimum aerodynamic designs. Over the past years, major studies were devoted to the classical benchmark of an optimal aerodynamic design for a 2D airfoil, where the main focus was on proper geometry parameterization and selection of an efficient optimization algorithm. For instance, Fanjoy and Crossley [2] developed a method to optimize airfoil designs by using 21 design variables representing the control points of a B-spline. This appears to be sufficient to reproduce nearly any arbitrary shape, but introduces geometric waves between control points translated to "wavy" velocity distribution in the analysis. A similar approach with 10 control points was employed by Pulliam et al. [3] in their comparison of genetic and adjoint methods for viscous airfoil optimization. Alternatives to the direct-design approach, including inverse methods to parameterize the geometry by matching it to the optimal flowfield conditions, were also developed [4]. For rotorcraft airfoils, a study on aeroacoustic optimization using a genetic algorithm was conducted in Ref. [5]. Using simplifying assumptions for low-order aeroacoustic analysis without structural constraints, a set of rotor airfoil shapes was generated representing a compromise between aerodynamic efficiency and minimum noise. Among the generated shapes, airfoils with *waves* on the upper and lower surfaces were predicted to produce reduction in the overall sound-pressure level. For 3D geometries, several recent works (e.g., Refs. [6-7]) addressed optimal wing and aircraft configurations, some using a multiobjective optimization strategy, and increasingly relying on evolutionary algorithms. Various methods to parameterize 3D geometries were analyzed, typically resulting in a large number of design variables to adequately represent the optimized shapes in terms of Bezier surfaces or B-splines. In one such study [8], a fuselage of a supersonic transport was parameterized in terms of 37 Bezier polygons, resulting, for an integrated wing-fuselage configuration, in 131 design variables.

---

\* Graduate Research Assistant (idahosau@erau.edu)

[†] Associate Professor, Senior Member of AIAA (golubd1b@erau.edu)

‡ Senior Engineer, Senior Member of AIAA (vladimir@vrand.com)

Various works also discussed automated grid generation procedures.

Increasingly, the multiobjective optimization studies have been including a noise metric as a component of their objective functions. This is particularly the case for a supersonic transport design where optimal shapes where developed to lower the sonic boom strength (e.g., Ref. [8]). In general, noise as a factor may be accounted at multiple levels in aircraft systems design. In a preliminary design for innovative complete aircraft configurations, the approach may involve first identifying the dominant sources of noise radiation that, in the aircraft MDO study, could be included in the cost function in the form of a noise metric [9, 10]. Such optimization problems, once properly posed, may lead to very unusual configurations provided the noise metric represents a highly weighted cost function component. For instance, a conceptual search in Ref. [11] for a "functionally-silent" aircraft configuration (with up to 30 dB overall noise reduction) has shown promise of a blended-wing-body concept with innovations including ultra-high bypass ratio turbofan engines and distributed propulsion system. One common feature of such studies is that they illustrate the need to develop a comprehensive noise assessment framework in order to address a problem of multiobjective aeroacoustic optimization with sufficient confidence.

The design of highly efficient and quiet turbomachinery and generally propulsion system components represents a most difficult and challenging task in many industrial applications ranging from aeropropulsion (e.g., turbofan and turboprop engines) to automotive and air-conditioning industries (e.g., cooling fans). The challenge is presented by the variety of flow and geometric parameters affecting the aerodynamic and acoustic performance, as well as the complexity of multi-scale unsteady flow-structure interaction phenomena leading to numerous noise-producing mechanisms and difficulty in their description and prediction. The accuracy and numerical efficiency of noise prediction techniques are critical factors in developing approaches to aeroacoustic geometry optimization studies. For that reason, very few examples of such studies exist (one example from Ref. [5] is mentioned above).

The current work addresses several critical issues related to the optimal aeroacoustic shape design in turbomachinery by examining them in the context of the automated, industry-like MDO environment, developed and distributed on a parallel high-performance computer cluster. In the following discussion, the main elements of such system are first examined to illustrate its various capabilities, particularly required to ensure a fully automated and efficient design optimization process. Next, two test studies related to optimal shape design of a rotor blade for low- and high-speed fan applications are discussed. In the first study, an attempt is made to employ a commercial CFD software coupled with an automated unstructured mesh generator. A procedure developed for proper parameterization of the blade geometry for optimal shape design is discussed, and could be found particularly useful in a variety of industrial turbomachinery applications that deal primarily with commercial CFD packages. In the second study, we employ aeroacoustic prediction methods to examine an approach to aeroacoustic shape optimization of a blade designed for high-speed rotor applications.

## COMPONENTS OF AUTOMATED MDO ENVIRONMENT

The main elements of any automated MDO environment can be roughly subdivided into three major categories [12]: (i) CAD Modeling; (ii) Grid Generation; (iii) Design and Optimization Tools (including response sensitivity analysis). Each of these categories has been a focus of intensive research activities in recent years, aimed, in particular, at establishing transparent links for integrating all components in one automated, robust design and optimization process. In general, the automated design systems must provide for the following capabilities [12]: (i) Use CAD for geometry creation; (ii) Generate grids automatically (black-box grid generation system); (iii) Use a common geometry representation for all disciplines involved in optimization process; (iv) Calculate analytical grid and geometry sensitivities; (v) Transfer data among disciplines consistently; (vi) Operate in an integrated system; (vii) Parameterize discipline models consistently. Below, we examine selected aspects of these features as they are implemented in our integrated system and further in test problems.

The essential elements of our industry-like, distributed, automated design optimization system include three software components developed by VR&D, Inc.: VisualDOC, GENESIS, and DOT [13]. The primary component in most design optimization procedures, VisualDOC, is a graphics-based, general-purpose design optimization software system designed to interface easily to third-party analysis programs using

its dedicated VisualScript interface. GENESIS is a fully integrated FEA and design optimization package providing design options of shape, sizing and topology optimization. Finally, Design Optimization Tools (DOT) is a library of software modules that is designed to help solve a variety of nonlinear constrained or unconstrained optimization problems (used in many existing design optimization products, such as GENESIS, VisualDOC, MSC/NASTRAN, ADAMS, FEM5, POLYFEM, DAKOTA). VisualDOC's structure includes a graphical user interface (GUI), a database, and several functional modules. The central part of the system is the object-rational, multi-user, platform-independent database acting as a container for all design information. GUI allows launching design tasks, performing real-time monitoring of the optimization process, and post-processing results for various forms of design variables that may be in continuous, integer, discrete, or any combination forms.

## Optimization Modules

The backbone of the optimization system is its functional modules performing the actual optimization, design study, etc. The menu includes the Gradient-Based Optimization (GBO), Design of Experiments (DOE), Response Surface Optimization (RSO), and Evolutionary Optimization (EO) modules.

GBO tools include extensively tested DOT software algorithms, such as sequential quadratic programming, modified method of feasible directions, sequential linear programming, Fletcher-Reeves, Broydon-Fletcher-Goldfarb-Shanno, and sequential unconstrained minimization technique methods, for various constrained and unconstrained multiobjective optimization problems. In the optimization process, VisualDOC calculates gradients of response-supplied cost functions and constraints using finite differences, but provides an option to employ user-supplied gradients.

Both DOE and RSO methodologies are used to establish empirical relationships between design variables and responses, which is a highly needed function in physical experiments and nonlinear analyses. They are also employed to filter out numerical noise from the analysis. According to Ref. [13], RSO has established itself as the most efficient method to use in optimization problems with relatively few (up to about 20) design variables, when the computational cost of performing a single analysis is high (a general trend in the growth of the number of terms in polynomial response surface models in shown in Figure 1). DOE works on the statistics of the design space distribution

thus helping to identify the design variables that have the most influence on the responses, and construct response surface approximations. A set of employed standard statistical DOE tools include full and fractional factorial, composite, simplex, Koshal, Box-Behnken, random, Latin Hypercube, Taguchi orthogonal arrays, D-optimal, and several other designs.
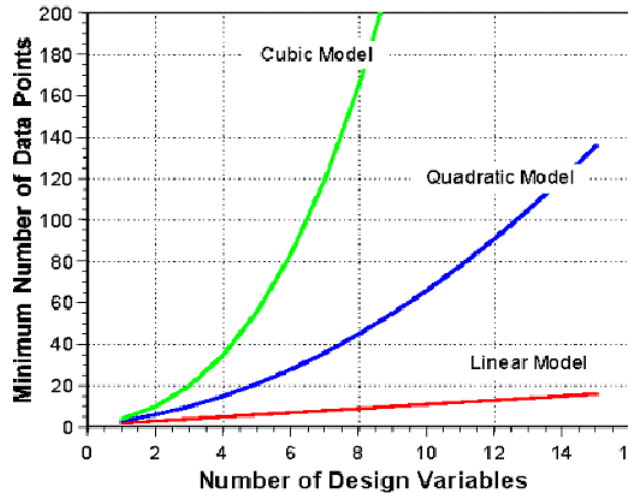


Figure 1: Influence of response surface models on number of design variables (courtesy VR&D, Inc.).

Finally, the Evolutional Optimization module includes Genetic and Particle Swarm Optimization algorithms, which benefits include better chances of finding global optima while not requiring gradient information, and good handling of numerical noise.

From the standpoint of the current test studies, one of the most important benefits of the system is its ability to efficiently interact with the third-party engineering analysis programs such as CFD and structural analysis tools. Such interaction is facilitated through a menu of interfaces, including ASCII-based Simple Text File Interface, multi-level Enhanced Text File Interface (VisualScript), and various specialized interfaces to MATLAB, Excel, and other analysis programs. Finally, another important VisualDOC's feature, for application to complex optimization problems, is the system's parallel computing capability. All the MDO functional modules, along with vectorized response analysis codes, have the ability to run in parallel on designated computer nodes using MPI message passing, thus creating a truly distributed environment. Although this feature has not been employed in the current benchmark tests, future studies will investigate effective use of the available networked cluster resources.

American Institute of Aeronautics and Astronautics

## CASE STUDY I: OPTIMAL AERODYNAMIC DESIGN OF LOW-SPEED FAN BLADE

The primary purpose of this project was to test the performance of the automated, distributed MDO/CFD environment designed for its future use in industrial turbomachinery MDO applications. In this study, we considered the task of optimal blade design to maximize the total efficiency of an axial fan with uniform upstream flow. Another goal of this project was to examine approaches to the efficient parameterization of the blade geometry that would be most appropriate for the robust automated MDO process. As mentioned above, contrary to the airfoil design studies, no guidelines have yet been established for the efficient parameterization of the blade geometry.

As a response analysis tool, we selected BladeGenPlus software component from CFX TurboPlatinum Package by ANSYS, Inc., since the latter is one of the primary commercial CFD analysis tools used in industrial turbomachinery design applications. BladeGenPlus is an integrated blade design software (BladeGen) coupled with blade passage unstructured RANS solver. The software was integrated with VisualDOC in the automated optimization process governed by VisualScript.

In the optimization process, the fan operating conditions were set either as specified parameters, or constraints in the optimization cycle, and included: (i) volumetric flow rate, (ii) range of safe (unstalled) fan operation, and (iii) fan static pressure rise. Fan diameter was usually prescribed as a geometric constraint. No structural constraints were imposed in this test study.

The initial task involved selection of proper parameters that completely and efficiently defined the fan blade geometry (this task is discussed in detail below). These parameters were then passed to the optimization module that generated another set of parameters describing a new, prospective blade design. At the next stages, the new blade geometry was generated in BladeGen, followed by automated unstructured mesh generation, CFD analysis, and transfer of results to the optimization module. Figure 2 illustrates a general flowchart of the optimization process. In summary, the optimization task can be roughly subdivided into four major segments: (i) Generation of blade geometry using BladeGen software based on current input parameters; (ii) CFD analysis performed on a new blade design using BladeGenPlus; (iii) Passing results of CFD analysis to VisualDoc optimizer; (iv) Generation of a new set of design parameters based on an iterative step of the selected optimization algorithm.
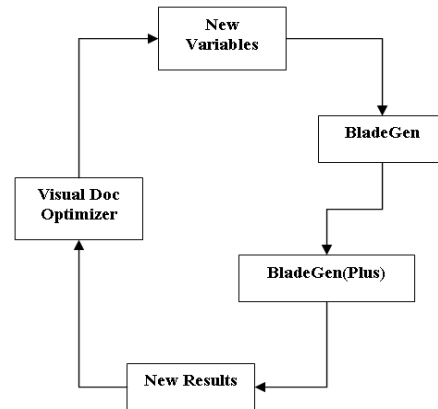


Figure 2: General MDO flowchart for Case Study I.

In what follows, we briefly describe some of the essential elements of this process and their functions.

### Parameterization of Blade Geometry

A critical step in the automated design optimization procedure was the selection of an efficient way to parametrically describe the blade geometry.
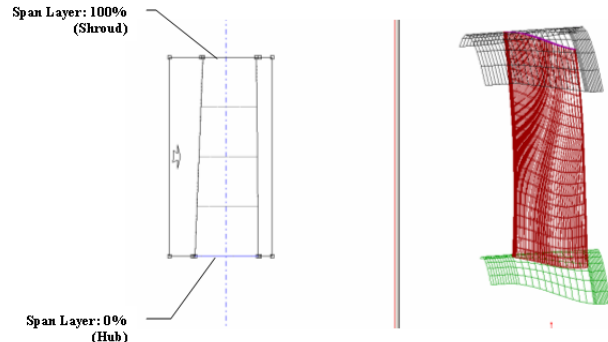


Figure 3: Definition of blade geometry in BladeGen.

In BladeGen, the blade model is defined by data points distributed over a number of user-specified constant-radius layers, spanning from 0% at the hub to 100% at the shroud. The geometrical properties, including blade angles and thickness distributions, are then specified at each spanwise layer, and interpolations between layers are employed to generate the three dimensional geometry, as shown in Figure 3.

The primary control parameters used in the blade geometry parameterization, include distributions of

4

blade angles $\theta$ and $\beta$. As evident from Figure 4, the two angles are interrelated, and thus only $\theta$–distribution is used as a design property, while $\beta$-distribution is specified based on variation of $\theta$. Note that according to the angles definition, the blade twist is determined by the spanwise $\beta$-distribution, while the blade sweep is prescribed by the spanwise $\theta$-distribution.
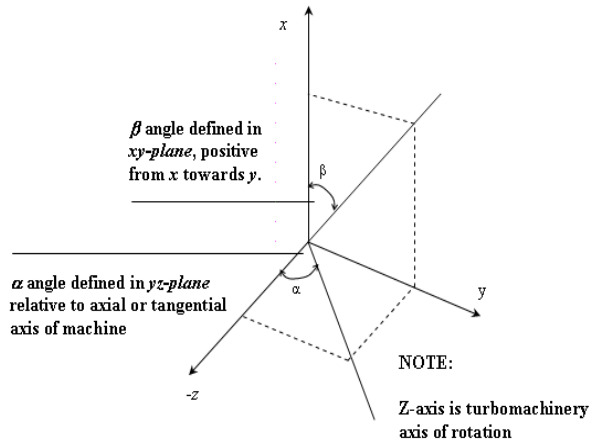


Figure 4: $\theta$ and $\beta$ blade angle definitions in BladeGen.

In the current approach, the initial blade design is parameterized using Bezier control points (connected by dotted segments in Figure 5) to define the chordwise $\theta$-distribution at each span layer. The use of Bezier points ensures a smooth $\theta$-distribution, free of discontinuities that could yield geometrically unfeasible blades. For example, in order to define $\theta$–distribution at the blade hub (span layer #1), the coordinates of 4 Bezier control points $(x\theta_{l,0}, y\theta_{l,0})$, $(x\theta_{l,1}, y\theta_{l,1})$, $(x\theta_{l,2}, y\theta_{l,2})$, $(x\theta_{l,3}, y\theta_{l,3})$ must be specified. The control Bezier points are used to generate both $\theta$ and thickness spanwise distributions, and employed as the primary geometrical design properties. The control design parameters are thus defined as $(x,y)$ pairs corresponding to 4 Bezier points that generate the blade shape distribution at each span layer, as illustrated in Figure 5.

In the test study, the span layers were evenly distributed from hub to shroud with a total of 5 span layers, and design variables were provided for each span layer for effective control of the blade geometry.

While the parameterization using Bezier curves provides smooth distribution of blade geometry at each
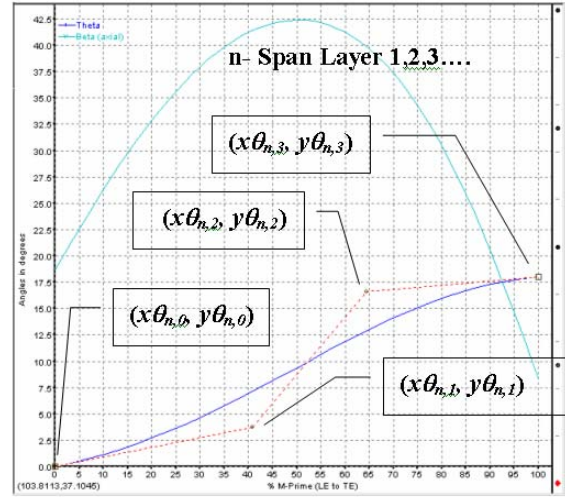


Figure 5: Chordwise blade angle variation.

span layer, the same quality has to be maintained for distribution of parameters responsible for spanwise variation of the geometry. To this end, the spanwise parameterization approach employed 3rd-order polynomials to define the radial distribution of the Bezier control points, resulting in a set of 4 polynomial coefficients as design control variables. For example, $\theta$- distribution at the blade leading edge is defined by the $(x\theta_{n,m}; y\theta_{n,m})$ pairs with 1≤n≤5 and $m=0$, where $n$ designates the span layers ($n=1$ is at the hub and $n=5$ is at the shroud), and $m=0$ corresponds to the leading edge. In the BladeGen notation, $x\theta_{n=1..5,0} = 0\%$ at the blade leading edge (for all span layers), and $x\theta_{n=1..5,3}=100\%$ at the blade trailing edge. Note that in the adopted parameterization scheme, the 3rd degree polynomials were only applied to prescribe the spanwise variation of $y\theta_{n,m=0..3}$ and $x\theta_{n,m=1}$ Bezier components. Figure 6 shows a sample radial polynomial distribution for $y\theta_{n,m}$ component (the abscissa corresponds to the radial coordinate). The coefficients of the 3rd order polynomials are thus selected as additional design control variables employed in the optimization of the blade geometry. For a total of 5 polynomial splines with 4 coefficients, 20 design variables are needed for proper parameterization of the blade geometry.

An additional constraint in the parameterization approach relates to one of the Bezier control points, $x\theta_{n,m=2}$. A careful analysis of the Bezier point specifications in Figure 5 suggests that the x-coordinate of the third control point ($x\theta_{n,m=2}$) must be placed after the x-coordinate of the second control point ($x\theta_{n,m=1}$) in

5

order to produce a geometrically feasible blade. Thus, a "distance factor" $d_{n=1..5}$ was introduced in order to deduce $x\theta_{n,m=2}$ Bezier components in terms of $x\theta_{n,m=1}$ and $x\theta_{n,m=3}$, using the following relationship:

$$x\theta_{n,m=2} = x\theta_{n,m=1} + (x\theta_{n,m=3} - x\theta_{n,m=1})d_n + 5,$$

with $0 \leq d_n \leq 0.95$. Thus, 5 additional design variables (one "distance factor" for each span layer) are needed for the complete parameterization of the 3-D blade geometry for $\theta$–distribution. In addition, as many as 10 Bezier components $x\theta_{n=1..5,0}$ and $x\theta_{n=1..5,3}$ could be added to the pool of possible design variables for additional control (but were held constant in the current test runs), bringing the total number of potential design control variables for parameterization of $\theta$-distribution to 35. Future work will investigate effects from various radial distributions including power, exponential and logarithmic laws that might provide a better approximation requiring fewer coefficients in describing the geometrical relationships, thus reducing the number of parameters required to describe the blade geometry.

The described parameterization procedure for $\theta$–distribution can be also applied to specify the blade thickness distribution, thus doubling the number of possible design variables. Thickness parameters were held constant in the current shape optimization studies, but their variation is a potential subject of future research.
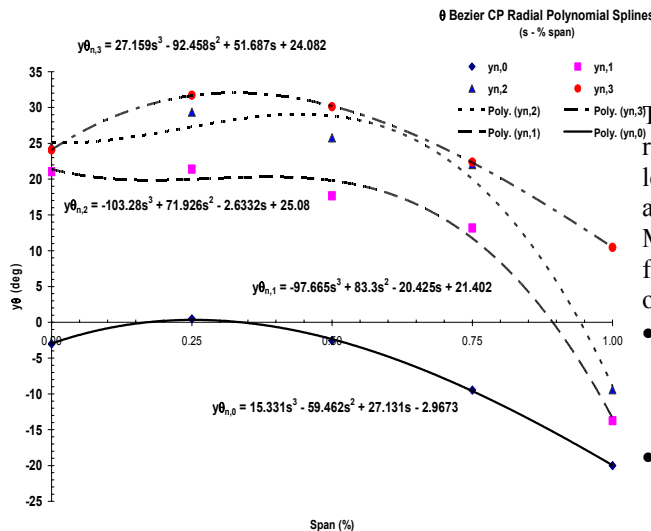


Figure 6: Bezier spanwise polynomial splines.

In addition to geometrical parameters, the number of design variables selected for passing to the optimization module included the number of fan blades and rotational speed, adding to a total of 72 possible optimization variables. Also included in the list of possible design variables were several constraint parameters used in various scripts to validate the blade geometry, as well as flags that allow the user to vary the parameterization scheme. A total of 118 potential design parameters were passed to the optimization module.

**Automated Response Analysis Procedure**
It is essential to maintain the response analysis stage as a completely automated, non-interactive segment of the optimization process. To this end, a set of batch executable utilities was implemented to accomplish the goal. In particular, the following BladeGenPlus utilities were employed:

- *BladeBatch* converted the optimizer-generated, ASCII-based blade model into a BladeGen design format;
- *BgBatch* applied new operating parameters such as the fan rotational speed and upstream flow conditions to the new BladeGen model;
- *BgGrid* generated unstructured blade-passage mesh for the new BladeGen model (Figure 7 illustrates a sample mesh for a single blade passage);
- *BgSolve* performed a CFD analysis of the blade passage and stored results in a specified file;
- *BgExtract* extracted computational results from the BgSolve output file and stored them in a specified file.

The need for completely automated optimization and response analysis procedures implies a considerable level of robustness to be built in the MDO environment, allowing it to handle extreme design cases. To this end, MATLAB scripts were developed to handle the following issues identified as critical to the robustness of the MDO methodology:

- Invalidity of extremely twisted, swept or distorted blade designs (as illustrated in Figure 8) is communicated to the optimization module through Geometry Pass/Fail parameter;
- Information on blade designs for which mesh could not be successfully generated is passed to the optimization module through Grid Pass/Fail parameter;
- Invalidity of CFD results stored in the response analysis file is communicated to the optimization module through CFD Pass/Fail parameter.
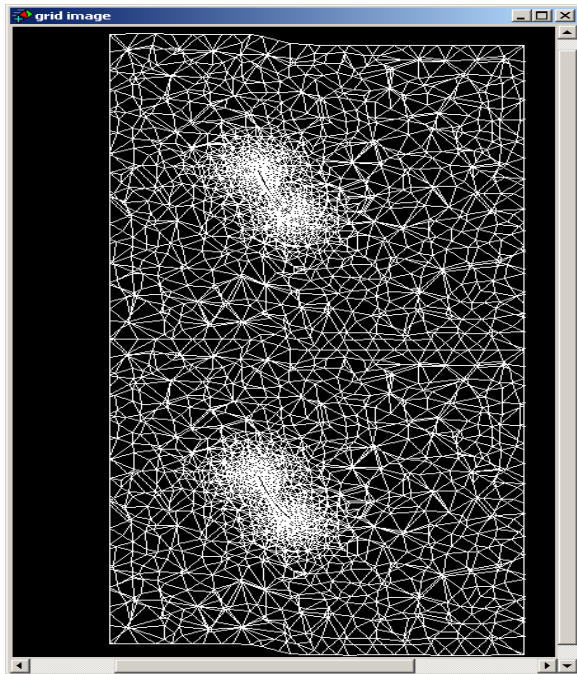
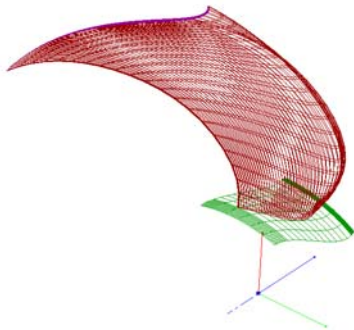Figure 7: Unstructured blade passage mesh from BladeGenPlus.



Figure 8: Highly swept blade design.

Note that the availability of the Pass/Fail parameter in VisualDOC, complemented by the software's ability to easily interface with MATLAB scripts, allows for a considerable robustness of the automated MDO process, as the latter is not immediately terminated in the event of problems associated with invalid blade designs, unsuccessful mesh generation, or unsuccessful CFD analysis (in all cases, the optimization process automatically recovers and continues).

The flowchart in Figure 9 summarizes details of implementation of various stages of the automated MDO/CFD procedure implemented in this case study.
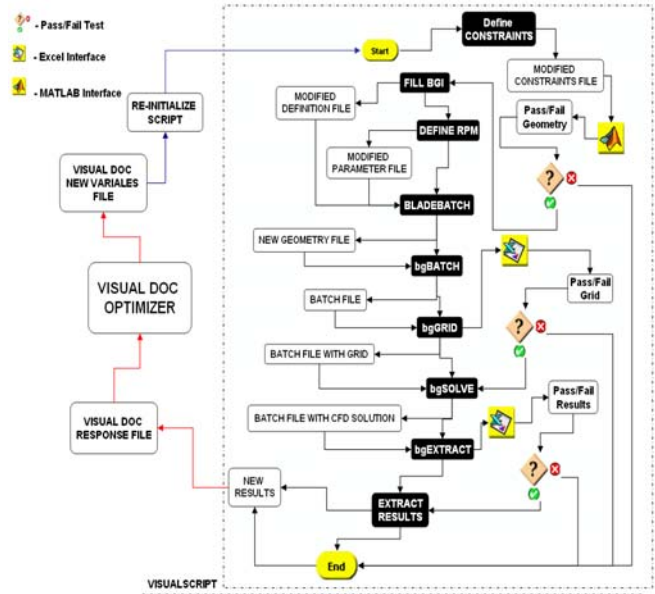


Figure 9: Detail flowchart of the design optimization process for Case Study I.

**Optimization Algorithms and Results**

In the optimization test runs, the design control parameters describing the blade geometry included 4 pairs of Bezier coefficients $(x_{n=1..5,0}, y_{n=1..5,0})$, $(x_{n=1..5,1}, y_{n=1..5,1})$, $(x_{n=1..5,2}, y_{n=1..5,2})$, $(x_{n=1..5,3}, y_{n=1..5,3})$ for $\theta$ and thickness distributions at 5 span layers, as well as the number of blades and fan rotational speed (RPM). Four original blade designs were used as "base" models (in Figure 10), with the primary purpose to validate the global convergence of the optimization process by starting from four distinct points of the design space. The concurrence between results of the optimization runs could serve as a measure of the "global nature" of the obtained optimal solution. Parameters of the initial blade models are shown in Table 1.

|  | Model1 | Model2 | Model3 | Model4 |
|---|---|---|---|---|
| RPM | 1140 | 1170 | 1140 | 1140 |
| Blades | 9 | 9 | 9 | 3 |
| Hub/Tip | 0.40 | 0.40 | 0.45 | 0.40 |

Table 1: Parameters of the initial blade models.

Several optimization algorithms were tested within a menu of VisualDOC's modules. In all the tests, the most promising results were obtained using the Response Surface Optimization (RSO) module. Design iterations that were started from parameters of Model 1

7

and Model 4 achieved the best optimal designs, with gains in the total aerodynamic efficiency reaching 15%. Figures 11 and 12 illustrate results obtained from the RSO optimization runs for Model 1.
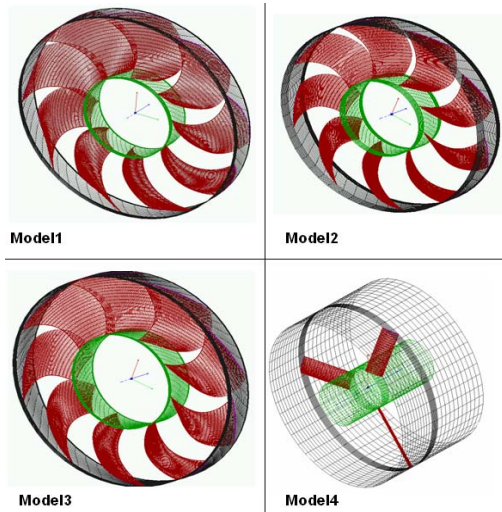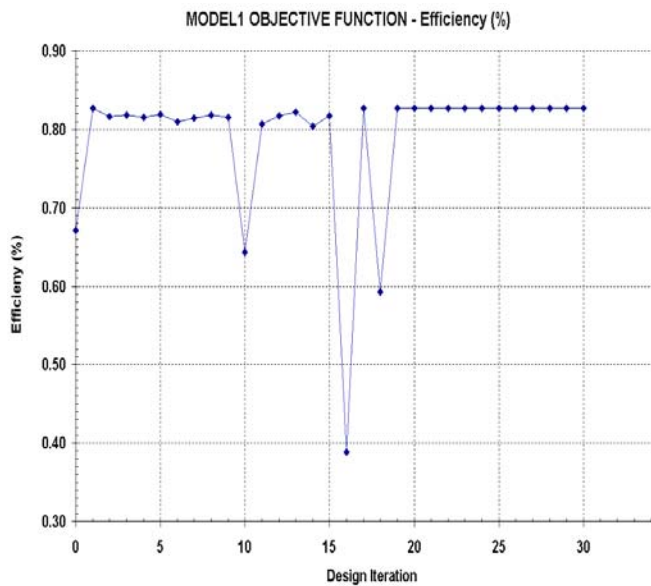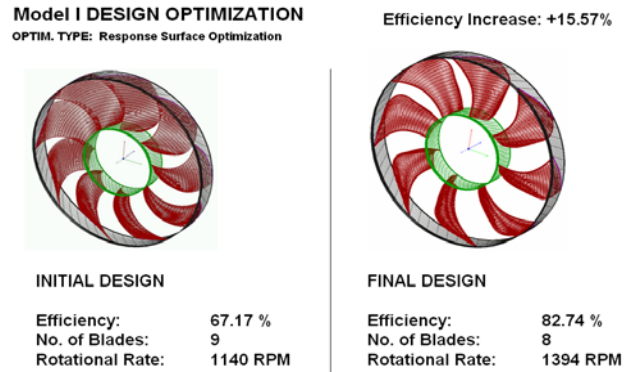


Figure 10: Base design models



Figure 12: Results of design optimization for Model 1.

In spite of certain success of these results, it is evident that the RSO algorithm was only able to achieve a local optimum, particularly since different base models led to different final designs. Unfortunately, the attempts to employ non-gradient-based methods, such as the Particle Swarm Optimization (PSO) algorithm, were unsuccessful due to extreme sensitivity of the automated mesh generator that was unable to handle radical design variations typical, e.g., of the PSO strategy (a similar trend and outcome were noted for test runs using the genetic algorithm).



Figure 11: History of objective function – Model 1.



Figure 13: Summary of design optimizations for different base models.

## Future Work

The next phases of this project could address several unresolved issues. First, the performance of non-gradient-based optimization schemes needs to be more thoroughly investigated. This includes a family of evolutionary algorithms, with increased number of blade parameters allowed to vary. The encountered difficulties in using such algorithms could be partially

American Institute of Aeronautics and Astronautics

resolved by re-visiting the blade geometry parameterization, and imposing more efficient constraints on allowed geometry variations. On the other side, the excessive sensitivity of BladeGenPlus unstructured mesh generator, that precluded such methods from being effectively tested, needs to be further explored. Finally, we plan to integrate our acoustic prediction capabilities in the optimization process. Several approaches to developing a noise metric to be included in the objective function may be investigated. One option is to select a control surface in the fan near-field where the CFD-resolved unsteady flow data can be extracted and propagated, using, e.g., a Kirchhoff surface code, to a chosen far field observer location, where the noise metric is then calculated. Another approach would be to focus on developing the metric based on predicting individual sources. For instance, the trailing edge noise alone may be targeted as the dominant broadband acoustic source. The integral solver predicting the trailing edge noise can be developed based on the RANS CFD solution output for turbulent flow properties along the blade surface (discussed, e.g., in Refs [14, 15]).

## CASE STUDY II: OPTIMAL AEROACOUSTIC DESIGN OF HIGH-SPEED PROPELLER BLADE

In this project, we tested the automated MDO system for future applications to aeroacoustic shape optimization of the blade geometry of a high-speed propeller or rotor. In the developed optimization process, the Aero/Acoustic Propfan Module (AAPM) code [16] was integrated with MDO environment as a response analysis tool.

The AAPM code predicts both aerodynamic performance and acoustic radiation of high-speed propellers with arbitrary blade geometry. The blade aerodynamic loading is computed using an unsteady, nonlinear panel method modeling propeller blades and evolution of their wakes. The acoustic predictions are obtained from an integral method that uses the aerodynamic results to calculate the propeller blade-passing frequency (BPF) harmonics corresponding to the dipole and monopole acoustic sources; the latter resulting from the blade aerodynamic loading and thickness distributions, respectively (the prediction algorithm closely follows a number of well-known works in the area of open-rotor acoustics, particularly Ref. [17]). The AAPM code was extensively tested for accuracy of aerodynamic and acoustic predictions against experimental data in Ref. [16]. It was developed for use in aeroacoustic optimization studies, and thus

employs an efficient geometry parameterization scheme that will be further explored in the future projects.

The current test study allowed to examine several optimization modules involved both in unconstrained and constrained design optimization processes. As usual, the selection of the objective function, imposed aerodynamic and geometric constraints, and design variables, was done in VisualDOC's input file, as illustrated in Figures 14 and 15. Design variables included the blade installation angle ($\phi_o$), the number of blades (*NBLADES*), tip diameter (*Diam*), and the blade rotational speed *(N)*. The ability to specify variable types as continuous, integer or discrete was particularly useful.

The optimal blade design was conducted with objective to minimize the blade noise metric, defined here as the first BPF harmonic at a fixed far-field observer position located in the plane of the propeller. The original blade model is depicted in Figure 16, and the "starting point" for design parameters in this study is shown in Table 2. The overall blade geometry was fixed in this test, along with the flight Mach number (0.32).

| Index | Name | Type | Objective | Low Bound | Initial Value | Upp Bound |
|---|---|---|---|---|---|---|
| 1 | NX | Constant ▼ | ☐ | None | 2.00 | None |
| 2 | INQ | Constant ▼ | ☐ | None | 1.00 | None |
| 3 | NBLADES | Integer ▼ | ☐ | 2.00 | 8.00 | 12.00 |
| 4 | PHIo | Continuous ▼ | ☐ | 20.00 | 34.45 | 60.00 |
| 5 | DIAM | Continuous ▼ | ☐ | 0.40 | 0.622 | 0.80 |
| 6 | ISI | Constant ▼ | ☐ | None | 0.00 | None |
| 7 | SWEEPR | Constant ▼ | ☐ | None | 45.00 | None |
| 8 | Mo | Constant ▼ | ☐ | 0.20 | 0.321 | 0.70 |
| 9 | N | Continuous ▼ | ☐ | 6000.00 | 8550.00 | 12000.00 |

Figure 14: Specification of design optimization variables in VisualDOC.

| Index | Name | Type | Objective | Constraint | Low Bound | Upp Bound |
|---|---|---|---|---|---|---|
| 1 | THRUST-kgf | Independent ▼ | ☐ | ☑ | 90.00 | None |
| 2 | CALFA | Independent ▼ | ☐ | ☐ | None | None |
| 3 | CETTA | Independent ▼ | ☐ | ☑ | 0.70 | None |
| 4 | POWER-hp | Independent ▼ | ☐ | ☐ | None | None |
| 5 | CBETA | Independent ▼ | ☐ | ☐ | None | None |
| 6 | LL | Independent ▼ | ☐ | ☐ | None | None |
| 7 | LT | Independent ▼ | ☐ | ☐ | None | None |
| 8 | LS | Independent ▼ | ☑ | ☐ | None | None |
| | | ▼ | ☐ | ☐ | | |

Figure 15: Specification of objective function and aerodynamic constraints in VisualDOC.

In the course of the design optimization run, the AAPM code was returning the propeller thrust, power (with their coefficients) and efficiency, that could be used as aerodynamic constraints, as well as the predicted

9
American Institute of Aeronautics and Astronautics

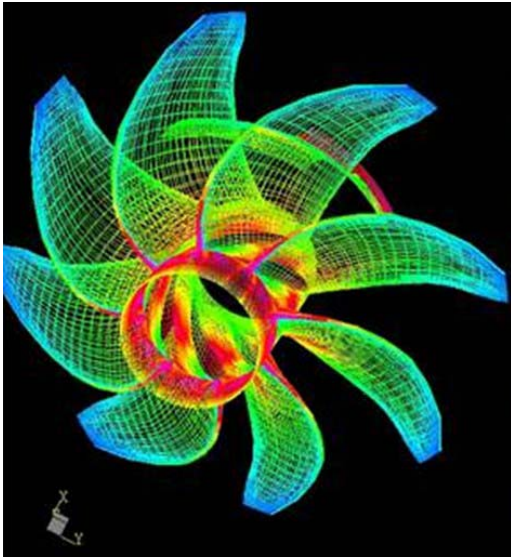loading (*LL*), thickness (*LT*) and total (*LS*) noise levels (Figure 15).



Figure 16: High-speed propeller model.

The optimization analysis was performed for two cases. In the first case, no limits were imposed on the design variables. The total noise level in decibels was defined as the objective function to be minimized in an *unconstrained* optimization process. In the second case, certain ranges for the variation of design variables were prescribed for the *constrained* optimization process. The limits imposed in the second case are detailed in Table 2.

| Variable | Lower Limit | Starting Point | Upper Limit |
|----------|-------------|----------------|-------------|
| NBLADES | 2 | 8 | 12 |
| $\Phi_o$(deg) | 20 | 34.45 | 60 |
| Diam (m) | 0.4 | 0.622 | 0.80 |
| N (rpm) | 6000 | 8550 | 12000 |

Table 2: Design parameters for constrained optimization run.

**Unconstrained Optimization**

The unconstrained optimization case was studied using the Fletcher-Reeves (FR) and Broydon-Fletcher-Goldfarb-Shanno (BFGS) gradient-based algorithms from the GBO module, and the Response Surface Optimization (RSO) algorithm. The non-gradient Particle Swarm (PSO) and genetic (GA) algorithms were not employed in the unconstrained studies, as both

require limits to be imposed on the optimization variables.

Figures 17-19 illustrate results from application of RSO algorithm that appeared more successful compared to others in this particular test. Note that the optimizer attempts to reduce the total noise level by first unloading the blade, which results in minimum thrust and power, and thus minimizes the loading noise component (*LL*) in Figure 19. The number of blades has increased that could result in higher *LT* component, but the trade-off is found by decreasing the propeller diameter and rotational speed, eventually bringing all noise components to a minimum. This test represents merely a "sanity" check for the performance of the automated optimization system, as, clearly, the results lack engineering sense when no constraints are imposed on the propeller aerodynamic performance.
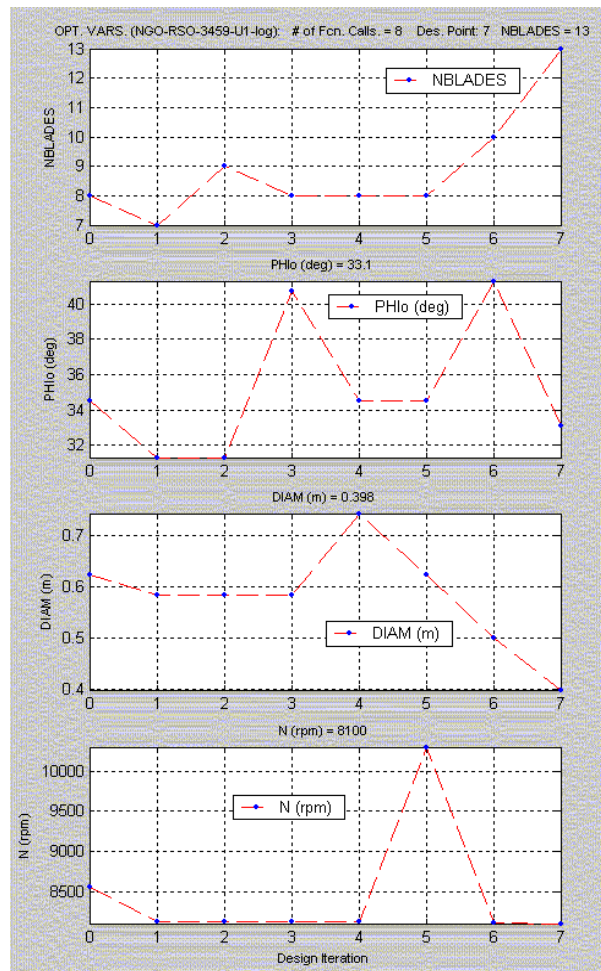


Figure 17: Unconstrained optimization using RSO algorithm: iteration history for design variables.
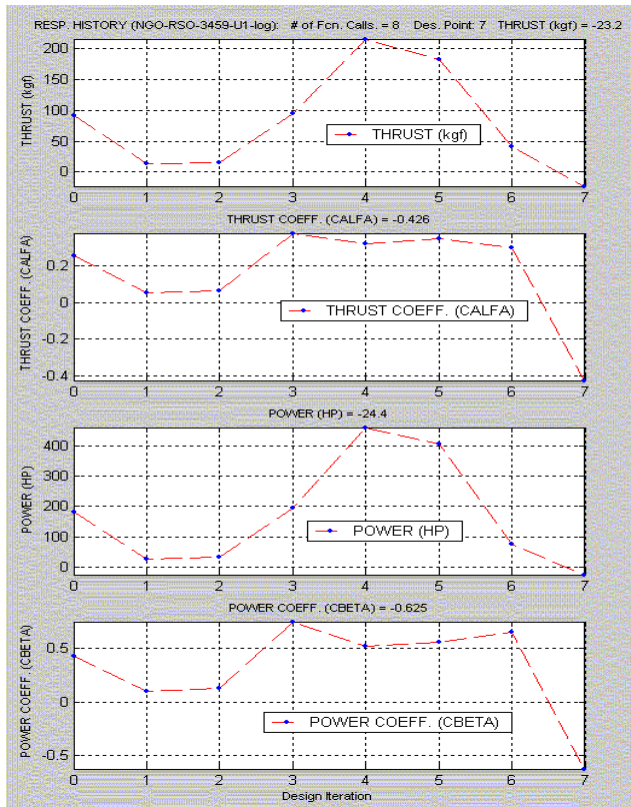
Figure 18: Unconstrained optimization using RSO algorithm: iteration history for thrust and power.



Figure 19: Unconstrained optimization using RSO algorithm: iteration history for efficiency and noise.

**Constrained Optimization**

The constrained optimization studies were performed using the GBO module's Modified Method of Feasible Directions (MMFD), Sequential Linear Programming (SLP) and Sequential Quadratic Programming (SQP) gradient-based algorithms, the RSO module, and the EO module's PSO and GA algorithms. In addition to limits on design variable shown in Table 2, lower bounds were imposed on the propeller efficiency and the amount of produced thrust, as indicated in Table 3.

| Parameter | Lower Bound |
|---|---|
| Efficiency ($\eta$) | 0.70 |
| Thrust (kg$_f$) | 90.00 |

Table 3: Constraints on aerodynamic performance.

These additional constraints were specified to investigate designs that could reduce total noise while maintaining the aerodynamic performance of the base model.
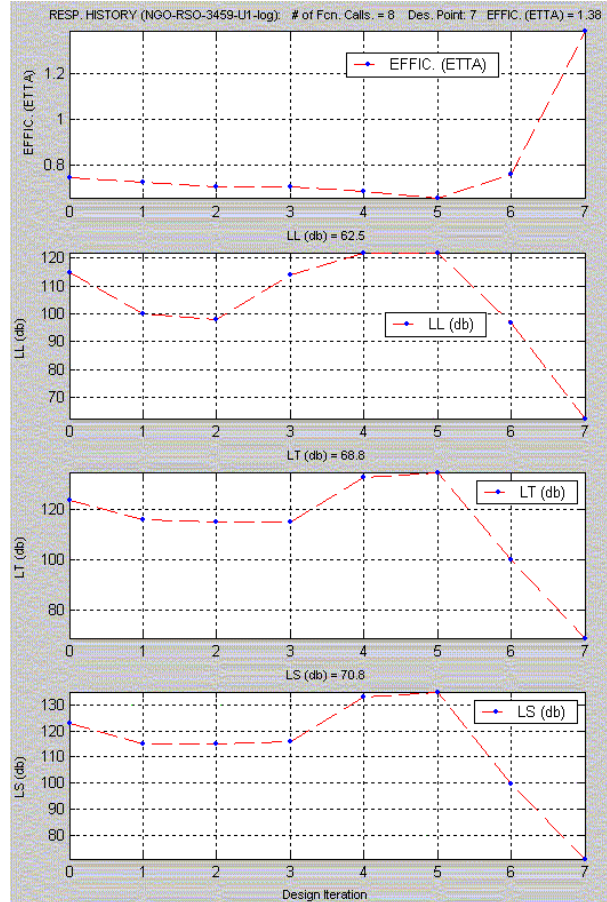
Figures 20-22 show the iteration history for design control variables, aerodynamic parameters, and produced noise, obtained using the best-performing PSO algorithm. A significant reduction of dB levels for all noise components (Figure 22) at the observer location is obtained by increasing the number of blades and blade installation angle, while decreasing the propeller rotational speed (Figure 20). Note that the aerodynamic constraints are also satisfied (Figures 21-22).

The overall performance analysis for those four of all tested algorithms that showed a noticeable improvement in the objective function (Table 4) suggests that, in general, the results varied significantly, with one exception of the gradient-based SLP algorithm that produced trends similar to PSO's results. One general trend that distinguished the performance of the evolutionary-type algorithms compared to the gradient ones was the ability of the former to operate on the complete range of design variables. For instance, all the
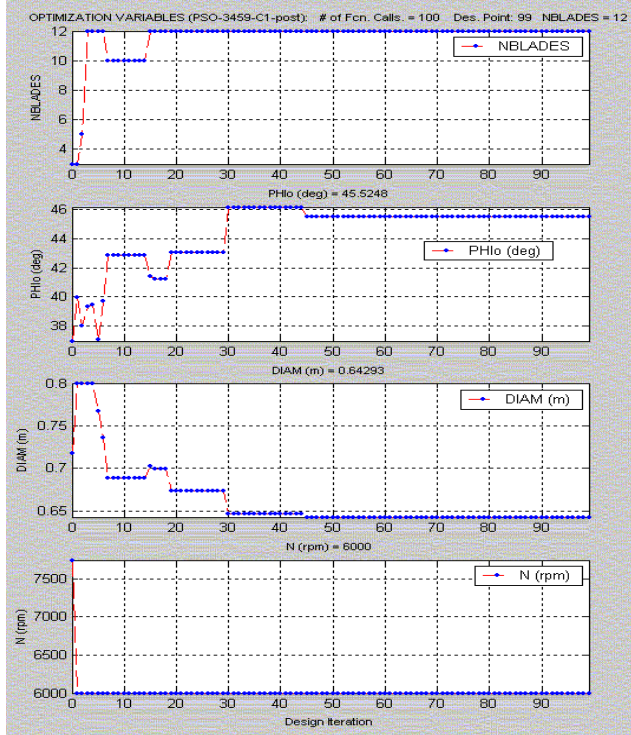
American Institute of Aeronautics and Astronautics

Figure 20: Constrained optimization using PSO algorithm: iteration history for design variables.



Figure 21: Constrained optimization using PSO algorithm: iteration history for thrust and power.

gradient-based optimization runs kept the number of propeller blades unchanged. For that reason only, SLP underperformed by 10 dB in total noise level reduction compared to PSO, still producing a better design than GA in just a few iterations. In general, the observed number of design iterations required to achieve the optimal design is a reflection of the typical non-linear increase in computational resources required for non-gradient based algorithms (compare the number of design iterations in Table 4).

Further benchmark studies on the algorithms' performance will be needed in order to more thoroughly investigate various tuning capabilities that are available in the menu of VisualDOC's options. Such tuning parameters could significantly improve the relatively poor results produced in the current test study by GA, RSO, and several tested gradient-based algorithms. The next stage of this project will also include new design variables that fully parameterize the blade geometry, for a more complete study of optimal aero/acoustic blade design.

**Future Work**
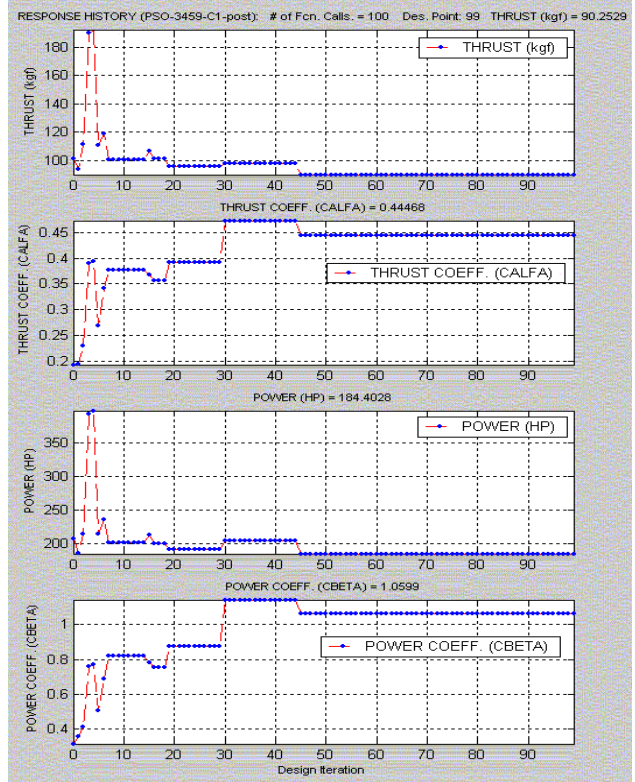In a modern high-bypass turbofan engine, the high-speed fan is a major source of noise radiation. On the other hand, a significant portion of the BPF tones (dominating in open-rotor configurations) is suppressed by the bypass duct. One of the remaining important mechanisms of the tonal noise production is due to Tyler-Sofrin modes caused by unsteady rotor-stator interaction phenomena. With the latter usually controlled by selecting proper blade counts and duct acoustic liners, the broadband sound spectrum caused by the blade "self-noise" acoustic sources becomes one of the dominant fan noise components. The fan broadband acoustic radiation is difficult to control, and thus one approach would be to separately investigate the blade geometry optimization specifically targeting the broadband acoustic sources. That will require adding new acoustic prediction capabilities to the database of response analysis tools, and changing parameters of the noise metric in the multiobjective optimization study. This again could involve exploring various existing models predicting, e.g., the blade trailing edge noise (for instance, in Refs. [14, 15]), that employ the turbulent boundary layer statistics in the form that can be either extracted from RANS or LES calculations, or obtained from an empirical database. Once validated, such models could be included in the optimization process either as separate acoustic
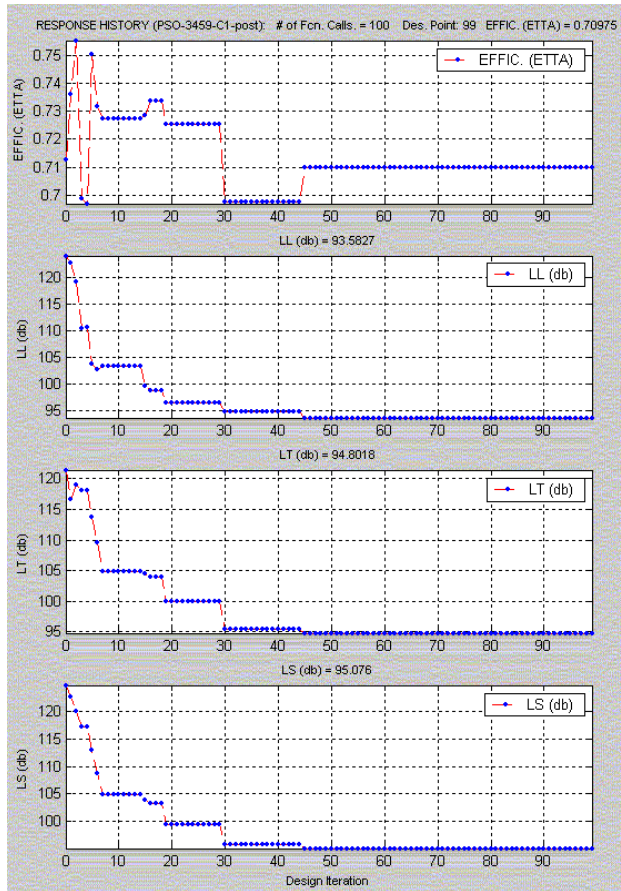
12
American Institute of Aeronautics and Astronautics

Figure 22: Constrained optimization using PSO algorithm: iteration history for efficiency and noise.

|  | Base Design | SLP | SQP | PSO | GA |
|---|---|---|---|---|---|
| **NBLADES** | 8 | 8 | 8 | 12 | 11 |
| **$\Phi_o$ (Deg)** | 34.45 | 46.96 | 40.37 | 45.52 | 35.00 |
| **Diameter (m)** | 0.6220 | 0.6431 | 0.5606 | 0.6429 | 0.8000 |
| **N (rpm)** | 8550 | 6007 | 8549 | 6000 | 6057 |
| **Thrust ($kg_f$)** | 92.25 | 89.97 | 90.04 | 90.25 | 113.10 |
| **Power (HP)** | 180.30 | 184.95 | 186.57 | 184.40 | 216.33 |
| **Efficiency ($\eta$)** | 0.7420 | 0.7054 | 0.6998 | 0.7098 | 0.7581 |
| **Loading Noise LL (db)** | 115.49 | 106.37 | 114.41 | 93.58 | 107.89 |
| **Thickness Noise LT (db)** | 123.93 | 101.51 | 115.99 | 94.80 | 119.24 |
| **Total Noise LS (db)** | 123.17 | 105.77 | 116.09 | 95.08 | 118.50 |
| **# of Design Iterations** |  | 8 | 7 | 100 | 60 |

Table 4: Constrained optimization: summary of results.

prediction modules, or in combination, e.g., with a RANS solver (such as BladeGenPlus) that could be used to compute the required turbulence parameters. The latter could also be employed for more accurate predictions of the blade aerodynamic loading, e.g., at transonic tip speeds. In a more complete optimization scheme, several acoustic modules, targeting both tonal and broadband noise components, could be coupled together to produce an integral noise metric accounting for noise radiation from various blade acoustic sources. Note that structural constraints can be efficiently incorporated in the process using another component of the optimization system, the GENESIS software. Finally, for a more efficient optimization process, the future work will also explore the parallel performance capabilities of the distributed MDO environment.

## SUMMARY

This work conducted two studies examining approaches to optimal blade design using the developed automated, industry-like multidisciplinary design optimization (MDO) environment. For low-speed fan applications, a commercial CFD software coupled with an automated unstructured mesh generator was employed as a response analysis tool in a constrained, automated design optimization process, with objective to maximize the fan static efficiency. A separate study examined an approach to blade shape optimization to minimize tonal noise radiation from a high-speed propeller, with the response analysis module developed on the basis of nonlinear panel method coupled with an integral acoustic solver. The studies examined success of various optimization algorithms, including gradient-based and evolutionary, in finding global minima of the corresponding objective functions. Thus, the projects

served as benchmarks for testing the performance of the developed MDO environment by addressing numerous issues in the automated optimization procedure, such as those related to proper geometry parameterization, algorithm selection, and transparent interconnections between different elements of the design optimization process.

## ACKNOWLEDGEMENTS

## REFERENCES

1. Jameson, A., "Essential Elements of Computational Algorithms for Aerodynamic Analysis and Design," NASA/CR-97-206268, 1997.

2. Fanjoy, D.W. and Crossley, W.A., "Aerodynamic Shape Design for Rotor Airfoils via Genetic Algorithm," J. of American Helicopter Society, Vol.43, pp.263-270, 1998.

3. Pulliam, T.H., Nemec, M., Holst, T. and Zingg, D.W., "Comparison of Evolutionary (Genetic) Algorithm and Adjoint Methods for Multi-Objective Viscous Airfoil Optimizations," AIAA Paper 2003-298.

4. Gardner, B.A. and Selig, S.S., "Airfoil Design Using a Genetic Algorithm and an Inverse Method," AIAA Paper 2003-0043.

5. Jones, B.R., Crossley, W.A. and Lyrintzis, A.S., "Aerodynamic and Aeroacoustic Optimization of Rotorcraft Airfoils via a Parallel Genetic Algorithm," Journal of Aircraft, Vol.37, 2000.

6. Cliff, S.E., Reuter, J.J., Saunders, D.A. and Hicks, R.M., "Single-Point and Multipoint Aerodynamic Shape Optimization of High-Speed Civil Transport," Journal of Aircraft, Vol.38, 2001.

7. Sasaki, D., Obayashi, S. and Nakahashi, K., "Navier-Stokes Optimization of Supersonic Wings with Four Objectives Using Evolutionary Algorithm," Journal of Aircraft, Vol. 39, 2001.

8. Sasaki, D., Yang, G. and Obayashi, S., "Automated Aerodynamic Optimization System for SST Wing-Body Configuration," AIAA Paper 2002-5549.

9. Hosder, S., Schetz, J.A., Grossman, B. and Mason, W.H., "Airframe Noise Modeling Appropriate for Multidisciplinary Design and Optimization," AIAA Paper 2004-698.

10. Morino, L., Iemma, U., Bernardini, G. and Diez, M., "Community Noise Considerations in Multidisciplinary Optimization for Preliminary Design of Innovative Configurations," AIAA Paper 2004-2809.

11. Manneville, A., Pilczer, D. and Spakovszky, Z.S., "Noise Reduction Assessments and Preliminary Design Implications for a Functionally-Silent Aircraft," AIAA Paper 2004-2925.

12. Samareh, J.A., "Geometry Modeling and Grid Generation for Design and Optimization," Keynote Lecture at ICASE/LaRC/NSF/ARO Workshop on Computational Aerosciences in the 21st Century, April 22-24, 1998.

13. Balabanov, V.O., Charpentier, C., Ghosh, D., Quinn, G., Vanderplaats, G., and Venter, G., "VisualDOC: A Software System for General-Purpose Integration and Design Optimization," AIAA Paper 2002-5513.

14. Moreau, S. and Roger, M., "Competing Broadband Noise Mechanisms in Low Speed Axial Fans," AIAA Paper 2004-3039.

15. Glegg, S.A.L., Devenport, W.J. and Spitz, N., "The Application of Proper Orthogonal Decomposition to Trailing Edge Noise," AIAA Paper 2004-2911.

16. Golubev, V.V., "Aeroacoustic Calculation of Propellers with Application of Discrete Vortices Method," in *Theoretical and Experimental Research of Selected Aerohydrodynamic Problems*, MFTI, Moscow, 1990 (in Russian).

17. Tam C.K.W. and Salikuddin M., "Weakly nonlinear acoustic and shock-wave theory of the noise of advanced high-speed turbopropellers," Journal of Fluid Mechanics, Vol. 164, 1986.